J. Fluid Mech. (1973), vol. 58, part 1, pp. 165–176
Printed in Great Britain

Scale diagrams for forced plumes

By B. R. MORTON AND JASON MIDDLETON
Department of Mathematics, Monash University, Melbourne

(Received 25 September 1972 and in revised form 11 January 1973)

A wide range of behaviour for turbulent forced plumes generated by vertical emission of heated or other buoyant fluid from finite sources in extensive and otherwise still uniform environments can be represented on a single non-dimensional diagram of characteristic heights, plotted against a parameter Γ, which for forced plumes represents the balance of flow conditions imposed at the physical source. The set of curves presented includes the maximum height of ascent for negatively buoyant plumes, and the height of transition from jet-like to plume-like behaviour above sources emitting buoyant fluid with excess momentum. The levels of various point and planar virtual sources are displayed also for comparison with earlier solutions. This *scale diagram* relates ascent and transition heights to the initial conditions at actual sources, in contrast to earlier presentations which have unduly emphasized virtual sources.

A *scale diagram* for maximum ascent heights in stably stratified environments permits choice of the range of source conditions for a specified height of ascent and ambient stratification.

1. Forced plumes in a neutral environment

An earlier paper (Morton 1959, referred to hereafter as I) described a treatment for turbulent forced plumes generated from steady sources emitting prescribed fluxes of mass ($\pi\rho_0 W_0$), momentum ($\pi\rho_0 V_0^2$) and heat or buoyancy ($\pi\rho_e F_0$), where ρ_e is the ambient density and ρ_0 the plume density at the source level $x = 0$. The model has obvious deficiencies, but there is reasonable evidence that it can give useful results in appropriate situations, and it is often helpful in obtaining at least a first estimate for the behaviour of plumes over real sources. The original solution, however, emphasized virtual sources to the extent that separate calculations were needed to relate an actual source to its equivalent virtual source. Such an emphasis of idealized virtual sources may be economical but confusing, and it appears to have led some authors (e.g. Telford 1966) to underestimate the range of source conditions covered. These include three regimes of behaviour: (i) negatively buoyant jets of heavy fluid projected upwards ($\Gamma < 0$); (ii) positively buoyant jets of light fluid projected upwards with initial velocity exceeding that of the corresponding simple plume ($0 < \Gamma < 1$); and (iii) positively buoyant jets with initial velocity less than that of the corresponding simple plume ($1 < \Gamma$). The limiting case $\Gamma = 1$ corresponds to the simple plume from a virtual source of buoyancy only (at prescribed depth below the actual source), and $\Gamma = 0$ to the hypothetical case of a source of zero radius at $x = 0$ (the actual source level), which has $W_0 = 0$ necessarily and includes the limiting cases of (i) and (ii) as negatively and positively buoyant forced plumes from 'actual point sources'. It includes also the ideal neutral jet $\Gamma = 0$ with $F_0 = 0$ and $W_0 = 0$ (but $V_0 > 0$), but *jets* from real sources ($F_0 = 0$, $W_0 > 0$ and $V_0 > 0$) are best regarded as excluded. In the former case 'real' and virtual sources coincide at $x = 0$ and the depth to the virtual source is obtained from that for the general forced plume $x_{vs} = x_{vs}(\Gamma)$ as the limiting (but unrealistic) case $x_{vs} \to 0$ as $\Gamma \to 0$. In the latter case, however, the depth of the virtual source is determined by W_0/V_0 and not by Γ, and in this representation simple jets comprise a branch family $\Gamma = 0$, $x_{vs} \propto W_0/V_0$. The dimensionless parameter Γ, defined below, provides a measure of the relative effects of mass, momentum and buoyancy flux from the source. The range of solutions can be displayed clearly by the construction of a *scale diagram*, showing the variation with Γ of various characteristic lengths, in each case for actual sources at the level $x = 0$.

The following discussion is concerned largely with a re-interpretation of the solution derived in I and should be read in conjunction with that paper; only a brief summary will be given of the earlier results on the supposition that readers wishing to use this material will first become familiar with the earlier solution. For a more recent discussion of other aspects of plume behaviour see Turner (1969) and Morton (1971).

In I axisymmetric plumes, referred to cylindrical polar co-ordinates (X, R, ϕ) with origin O at the source centre and OX vertically upwards, were assumed to have Gaussian profiles of mean vertical velocity $u = U(X)\exp(-R^2/b^2)$ and mean buoyancy $g(\rho_e - \rho) = \rho_e P(X)\exp(-R^2/\lambda^2 b^2)$, where $b(X)$ and $\lambda b(X)$ are characteristic (radial) length scales for the two profiles. For thermally buoyant plumes $\rho_e - \rho = \rho_e \beta(T - T_e)$. Gross conservation equations are obtained by integrating the field equations representing local conservation of mass (subject to the Boussinesq approximation), vertical momentum and heat over horizontal sections of the forced plume, $X =$ constant, in the form

$$\frac{d}{dX}\int_0^\infty Ru\,dR = -[Rv]_0^\infty,$$

$$\frac{d}{dX}\int_0^\infty Ru^2\,dR = \beta g\int_0^\infty R(T - T_e)\,dR,$$

$$\frac{d}{dX}\int_0^\infty Ru(T - T_e)\,dR = -\frac{dT_e}{dX}\int_0^\infty Ru\,dR.$$

The quantity $-[Rv]_0^\infty$ represents the rate of entrainment or rate at which the plume absorbs ambient fluid per unit height, and this must be related to the other variables in order to obtain closure of the system of equations. I was based on the assumption that the plume is in a state of fully self-similar flow, in which case both fluctuating and mean velocities scale together and entrainment can be characterized by an entrainment velocity of like scale, which may be taken as $\alpha U(X)$, where α is the entrainment constant. If the flow is not fully self-similar then α will not be a constant for all forced plumes, and there is some evidence that this is the case. However, little progress has been made in understanding the mechanisms of entrainment and there is at present no justification for using a more complicated entrainment model; as a result there is some uncertainty in the appropriate value for α, though this is likely to have only a limited effect on the results obtained here because of the way in which α enters the formulae.

Under the transformations

$$V = 2^{-\frac{1}{2}}bU, \quad W = b^2U, \quad F = \lambda^2(1+\lambda^2)^{-1}b^2UP,$$

and

$$F = F_0, \quad V = V_0 v, \quad W = 2^{\frac{3}{4}}\alpha^{\frac{1}{2}}(1+\lambda^2)^{-\frac{1}{2}} V_0^{\frac{5}{2}}|F_0|^{-\frac{1}{2}} w,$$
$$X = 2^{-\frac{3}{4}}\alpha^{-\frac{1}{2}}(1+\lambda^2)^{-\frac{1}{2}} V_0^{\frac{3}{2}}|F_0|^{-\frac{1}{2}} x,$$

the gross conservation equations reduce to the non-dimensional forms

$$dw/dx = v, \quad dv^4/dx = w \operatorname{sgn} F_0,$$

together with the condition of constant heat flux $F \equiv F_0$. Subject to source conditions $F = F_0$, $V = V_0$, $W = W_0$ at $X = 0$, or alternatively $v = 1$, $w = 2^{\frac{3}{2}}\,5^{-\frac{1}{2}}|\Gamma|^{\frac{1}{2}}$ at $x = 0$, these equations have parametric solution

$$w = \{\tfrac{8}{5} \operatorname{sgn} F_0(v^5 + \Gamma - 1)\}^{\frac{1}{2}},$$

$$x = 10^{\frac{1}{2}} \operatorname{sgn} F_0 \int_1^v \frac{v^3\,dv}{\{\operatorname{sgn} F_0(v^5+\Gamma-1)\}^{\frac{1}{2}}} \geqslant 0,$$

where

$$\Gamma = 5(1+\lambda^2)\,F_0 W_0^2/2^{\frac{9}{2}}\alpha V_0^5$$

is the forced-plume parameter for the source of strength (F_0, V_0, W_0) in a uniform environment, which in the form $4\alpha\Gamma/5\lambda^2 = b_0 P_0/U_0^2$ may be interpreted as the inverse square of a Froude number. Emission from the source is assumed to be upwards in all cases considered (with $V_0 > 0$ and $W_0 \geqslant 0$), and $\operatorname{sgn}\Gamma = \operatorname{sgn} F_0$. Plumes directed downwards have $V_0 < 0$ and that family of solutions can be obtained by obvious sign changes.

It has been shown in I that for a uniform environment the forced plume above a finite source (F_0, V_0, W_0) at $X = 0$ is the same as the part $X > 0$ of a corresponding plume with virtual (point) source $(F_0, \gamma V_0, 0)$ at $X = X_{vs}$, where $\gamma^5 = 1 - \Gamma$ and the virtual source is below the real source except for 'hot, lazy plumes' released with low source velocities. Thus the flow above a general source can always be related to a forced plume from a point source with modified strength and position, though the validity of the comparison will be poor for plumes of moderate or small aspect ratio (total height above the real source measured in source diameters). Such plumes behave like jets near their virtual sources and like simple plumes at rather larger distances. The transition from jet-like flow with $db/dX = 2\alpha$ to plume-like flow with $db/dX = \frac{6}{5}\alpha$ is illustrated in figure 1 for the limiting case $\Gamma = 0\ (F_0 \neq 0)$ of a positively buoyant forced plume with a point source $(F_0, V_0, 0)$ at $X = 0$. Turbulent jets have a larger spread angle or higher relative rate of spread than turbulent plumes (as is shown in figure 1 by a dotted line representing jet spread and a dashed line for asymptotic plume spread). The rate of spread at any level of a turbulent core flow depends on the local rates of change of volume or mass flux and of axial velocity; the former depends on the local rate of entrainment, while the latter depends both on the deceleration of plume fluid as a result of momentum sharing with entrained fluid and any buoyant acceleration. For a

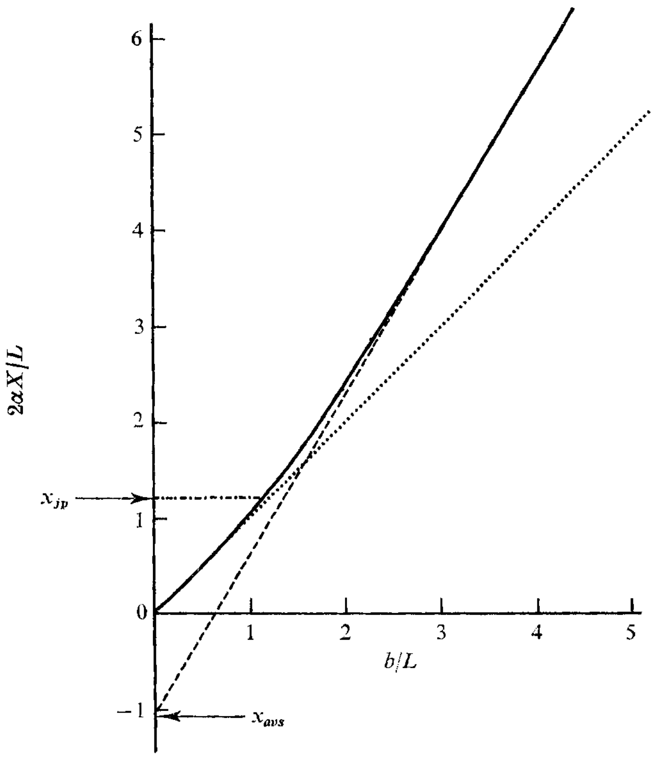

FIGURE 1. The lateral spread of a forced plume from the point source $(F_0, V_0, 0)$ with $\Gamma = 0$ at the origin plotted in the stretched dimensionless co-ordinates $(2\alpha X/L,\ b/L)$ to accentuate the rate of spread. The 'real' and virtual sources coincide at $x_{vs} = 0$; the asymptotic jet is marked by the dotted line, and the asymptotic plume with asymptotic virtual source at $x_{avs} = -1{\cdot}06$ by a dashed line; the level of transition from jet-like to plume-like behaviour $x_{jp} = 1{\cdot}20$ is indicated by a dash–dot line. F_0 is non-zero.

plume $d(b^2U)/dX = 5b^2U/3X$ and $dU/dX = -U/3X$, whereas for a jet $d(b^2U)/dX = b^2U/X$ and $dU/dX = -U/X$; and it is apparent that the much lower deceleration of the plume plays an important role in its reduced rate of spread. Thus a jet may be regarded as suffering a higher rate of dynamic decay axially than a plume because it has no continuing source of momentum generation. In general jets have a higher velocity than plumes in an important neighbourhood of the source and are more efficient at mixing with their environments, whereas plumes are better at transporting source fluid to large distances from the source. These differences are important in planning the dispersion of pollutants. The fact that plume spread depends both on entrainment and axial deceleration is important also in understanding the behaviour of jets of various gases in air.

The solution represented in figure 1 is a special case in that the virtual point source coincides with the actual source ($X_{vs} = 0$). Other significant levels indicated are the jet/plume transition at X_{jp}, taken as the level at which $db/dX = \frac{8}{5}\alpha$, intermediate between the asymptotic jet and plume values, and the virtual source corresponding to the asymptotic simple plume, at X_{avs}. The position of X_{jp} relative to the real source ($X = 0$) in more general cases is of interest as it provides

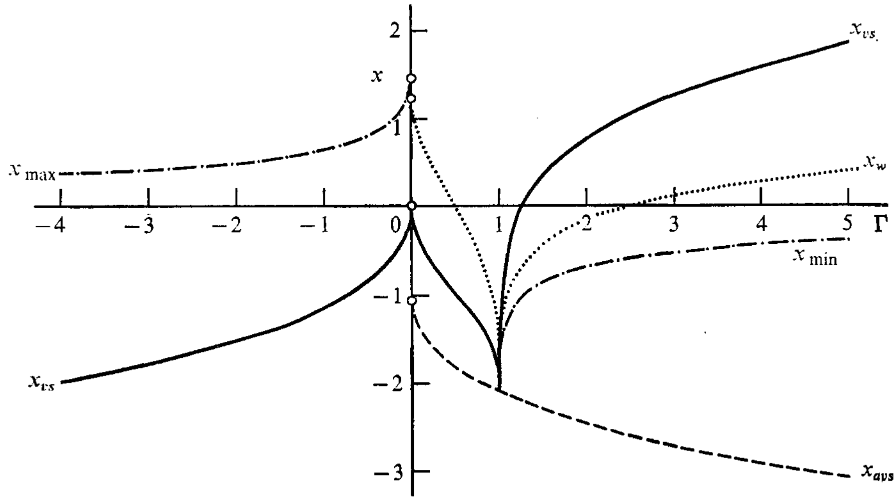

FIGURE 2. A scale diagram for the ascent of forced plumes in a uniform environment showing heights of representative plume features plotted against the non-dimensional parameter Γ, which provides a measure of the relative effects of buoyancy, mass and momentum flux from the source. The various curves mark the levels: ——, x_{vs} of the virtual point source ; - - - -, x_{avs} of the asymptotic virtual source; ⋯⋯, x_{jp} of the transition from jet-like to plume-like behaviour ($0 < \Gamma < 1$) and x_w of the 'waist' or level of minimum plume width ($1 < \Gamma$); —·—·—, x_{max} of the greatest height of ascent of negatively buoyant plumes. ($\Gamma < 0$) and x_{min} of the equivalent virtual planar source having fluxes of buoyancy and mass but not of momentum ($1 < \Gamma$). In every case the actual physical source is at the level $x = 0$.

a measure of the height through which the forced plume is inertially driven before buoyancy begins to dominate. The length scale

$$L = 2^{\frac{1}{4}}\alpha^{\frac{1}{2}}(1+\lambda^2)^{-\frac{1}{4}}|V_0|^{\frac{3}{4}}|F_0|^{-\frac{1}{2}}$$

arises naturally in the reduction of the equations for forced plumes and applies equally to light or heavy fluid projected upwards; in the former case it is proportional to the transition height $X_{jp} = 0{\cdot}60\alpha^{-1}L$ above the *virtual* source, and in the latter case to the maximum height X_{max}.

2. A scale diagram for neutral environments

The heights of virtual sources, transition levels, maximum heights and other levels representative of the flow behaviour may be collected together into a single *scale diagram* for a wide range of forced plumes. One such diagram is shown in figure 2, supported by figure 3, showing selected profiles in the following three regimes.

(i) $\Gamma \leqslant 0$: *negatively buoyant forced plumes generated by upward emission of fluid denser than its environment*

The source fluid rises to a maximum height $X_{max} \equiv Lx_{max}/2\alpha$ marked by the dash–dot curve from virtual point sources $(F_0, \gamma V_0, 0)$ at height $X_{vs} \equiv Lx_{vs}/2\alpha$ shown by the continuous curve. The maximum heights of ascent in this case

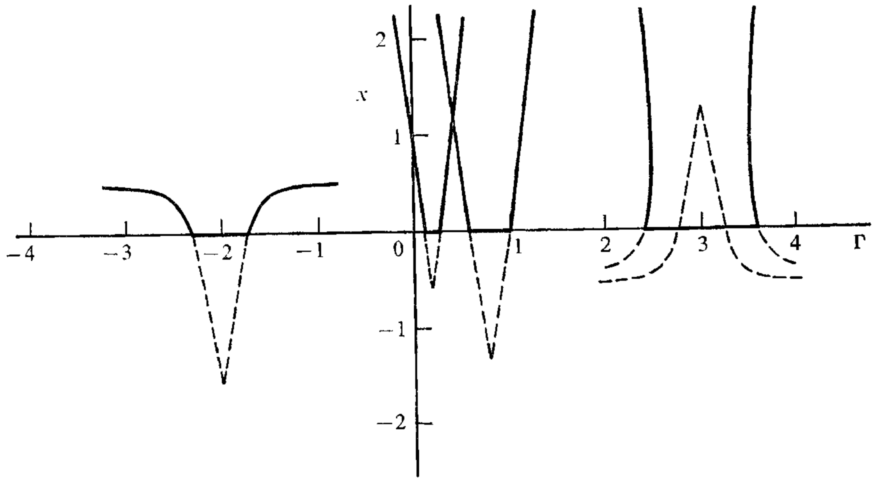

FIGURE 3. Typical plume profiles in the vertical. These cases correspond to the source and other levels of figure 2, and include: (i) $\Gamma = -2$, where the negatively buoyant plume suffers rapid deceleration and reaches a maximum non-dimensional height of 0·50; (ii) $\Gamma = 0{\cdot}2$, where the plume rises indefinitely (positively buoyant plume in a uniform environment) and has the largest initial rate of spread; (iii) $\Gamma = 0{\cdot}8$; with a slightly smaller initial rate of spread; (iv) $\Gamma = 3{\cdot}0$, where there is initial acceleration of plume with reduction of radius. In each case the actual source is at $x = 0$ and the relationship between actual and virtual sources is illustrated by broken curves.

are approximate only and might be thought an overestimate since this solution assumes laterally diverging flow at $X_{\max}$ with entrainment wholly from the environment, whereas the actual flow falls back towards the source level rather than diverging and partially shrouds the rising plumes with the result that at least some of the denser descending fluid will be re-entrained (but see Abraham (1967) for a comparison of theoretical models with experimental observations, suggesting that this $X_{\max}$ is too small). The limiting case $\Gamma = 0$ of a heavy upward-forced plume has $x_{vs} = 0$ and $x_{\max} = 1{\cdot}45$.

(ii) $0 \leqslant \Gamma \leqslant 1$: *positively buoyant forced plumes generated by upward emission of light fluid with excess velocity relative to the simple plume*

These forced plumes have an excess flux of source momentum relative to a simple plume and may tend initially towards jet-like behaviour, but revert to plume-like behaviour with increasing height as the proportion of momentum flux generated by buoyancy increases. The virtual source level x_{vs} is again shown by the continuous curve, and the jet/plume transition level x_{jp} by the dotted curve. Plume fluid in this case continues to rise, ultimately as a simple plume with the asymptotic virtual source at x_{avs} marked by the dashed curve. Limiting cases are the positively buoyant forced plume $\Gamma = 0$ from a point source at $x_{vs} = 0$ with $x_{jp} = 1{\cdot}20$, and the simple plume $\Gamma = 1$ with x_{vs}, x_{avs} and x_{jp} coincident at $-2{\cdot}11$. It may be noted that forced plumes exhibit appreciable tendencies towards jet-like behaviour near the actual source only for $0 \leqslant \Gamma < 0{\cdot}5$, and that these tendencies are strong only in the lower part of this range.

(iii) $1 \leqslant \Gamma$: *positively buoyant forced plumes generated by slow upward emission of light fluid relative to the equivalent simple plume*

These are 'lazy' plumes that need buoyant acceleration to reach their asymptotic flow state. In this range $\gamma < 0$, and the virtual (point) sources at x_{vs} shown by the continuous curve emit light fluid *downwards*; these descending (and, of course, quite hypothetical) sections of plume with negative buoyancy are analogous to those in case (i) and have lowest level of descent $x_{\min}$ (dash-dot curve). The formal solution indicates lateral outflow at this level, followed by return lateral inflow to produce an ascending positively buoyant plume with appreciable mass flux but low ascent velocity; continuing buoyant acceleration ultimately yields the asymptotic plume with asymptotic virtual source at x_{avs}, again indicated by the dashed curve. This regime can be regarded alternatively as being generated from the virtual (planar) source $\{F_0, 0, W_0(\Gamma-1)^{\frac{1}{2}}\,\Gamma^{-\frac{1}{2}}\}$ at the level $x_{\min}$ with zero momentum flux but finite fluxes of buoyancy and mass and infinite horizontal extent. At larger values of Γ the plume fluid suffers appreciable acceleration near the source as the buoyancy is strong but the entrainment rate small; this produces an initial narrowing of the plume to a waist of minimum radius at height x_w shown by the dotted line $(1 < \Gamma)$.

The variation of flow type with Γ can be illustrated further by plotting forced-plume profiles above the real source. Figure 4 shows a family of curves for the normalized plume radius b/b_s plotted against height x for Γ values ranging over the three different regimes; $b_s = 2^{\frac{3}{2}}5^{-\frac{1}{2}}|\Gamma|^{\frac{1}{2}}L$ is the plume radius at the source level $x = 0$. Lazy plumes with $1 < \Gamma$ suffer initial acceleration coupled with low rates of entrainment where velocities are small, and for $2{\cdot}50 < \Gamma$ exhibit 'waists' of reduced radius; $\Gamma = 1$ corresponds to the asymptotic rate of plume spread; as Γ is further reduced there is an increasing development region of jet-like flow; and for $\Gamma < 0$ the negative buoyancy causes deceleration with an increased spread rate. It may be noted that the x scale in figure 4 has been reduced relative to the b scale by a factor $(2\alpha)^{-1}$, or roughly 6: this enhances the apparent rate of spread and makes the figure easier to interpret.

3. Length scales

Two length scales have been introduced in the preceding discussion:

$$L = 2^{\frac{1}{4}}\alpha^{\frac{1}{2}}(1+\lambda^2)^{-\frac{1}{2}}\,V_0^{\frac{3}{2}}|F_0|^{-\frac{1}{2}}$$

and

$$b_s = 2^{\frac{3}{2}}5^{-\frac{1}{2}}|\Gamma|^{\frac{1}{2}}L.$$

Although L may be regarded as the primary scale for flow development in the axial direction, an observer would probably judge many flow phenomena in terms of the source radius b_s. In terms of the effective source radius b_s the appropriate vertical length scale is $X/x = L/2\alpha = b_s/2^{\frac{5}{2}}5^{-\frac{1}{2}}\alpha|\Gamma|^{\frac{1}{2}}$, and this scale provides a measure for the maximum height of ascent of a negatively buoyant forced plume in a uniform environment and for the height to jet/plume transition in the range $0 \leqslant \Gamma < 0{\cdot}5$, with coefficients of proportionality to be extracted from figure 2 for given Γ.

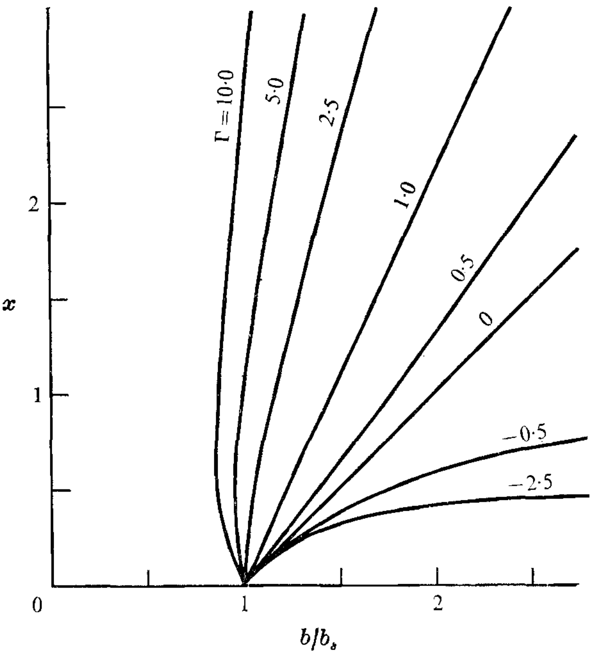

FIGURE 4. A family of forced-plume profiles showing the variation of radius (normalized with respect to source radius b_s) with height (x) for a range of values of Γ spanning the three main types of behaviour.

4. Forced plumes in stable environments

In a stably stratified environment the buoyancy flux decreases progressively with height as the plume rises into lighter surroundings, and such forced plumes become negatively buoyant in at least their upper regions and have bounded height of ascent. Profiles of velocity and buoyancy are likely to suffer modification as the fluid rises through the neutral level into the region of reversed buoyancy, and the self-similarity assumption is bound to be violated to some extent. For this reason the Gaussian profiles adopted in neutral environments will be replaced here by top-hat profiles which may be interpreted as rather simpler averages over the profile without imposed structure.

Gaussian profiles may be shown also to have certain undesirable properties in stable environments. In terms of thermal plumes in stable thermally stratified environments ($dT_e/dX > 0$), the plume must suffer net cooling and therefore decrease in temperature on ascent in regions where it is hotter than its immediate environment, and net warming with temperature increasing with ascent in the overshoot region where it is cooler than its environment: thus $\operatorname{sgn}[(T-T_e)\,dT/dX] = -1$ for $T-T_e \neq 0$, or the second law of thermodynamics will be violated. For *Gaussian profiles* of velocity $U(X)\exp(-R^2/b^2)$ and buoyancy $\rho_0 P(X)\exp(-R^2/\lambda^2 b^2)$ it may be shown from the relevant plume equations that

$$\frac{dT}{dX} = -\frac{1}{\lambda^2}\frac{dT_e}{dX} - \frac{2\alpha}{b}(T-T_e);$$

thus dT/dX remains negative through the level of neutral buoyancy and into the uppermost region of the plume, and from the original solution

$$\operatorname{sgn}[(T-T_e)\,dT/dX] = +1$$

throughout the upper region of reversed buoyancy. The corresponding expression for *top-hat profiles* of vertical velocity and buoyancy

$$u = \begin{cases} U(X), & 0 \leqslant R \leqslant b, \\ 0, & b < R, \end{cases} \qquad \rho = \begin{cases} \rho_0 P(X), & 0 \leqslant R \geqslant \lambda b, \\ 0, & \lambda b < R, \end{cases}$$

where $\lambda > 1$, is
$$\frac{dT}{dX} = -\frac{2\alpha}{b}(T-T_e),$$

and in this case $\operatorname{sgn}[(T-T_e)\,dT/dX] = \operatorname{sgn}(-2\alpha/b) = -1$ throughout the plume. Thus, although heat is being transferred appropriately from the point of view of plume average values, the Gaussian profile appears to provide an over-constraint on the temperature field by forcing an unduly large temperature deficit at the axis to achieve the correct axial heat flux. A similar difficulty is found with top-hat profiles having $\lambda < 1$, which again correspond to a concentration of heat towards the axis, although laboratory observations of Rouse, Yih & Humphreys (1952) appear to show that $\lambda > 1$ for axisymmetric thermal plumes. There is no cause for undue concern at this partial failure of the Gaussian profile for stable environments, as little physical significance for the particular form of profile adopted survives integration of the equations over a plume section. In spite of this, it seems appropriate to use top-hat profiles for stable environments here as in I.

In order that ascent heights in both neutral and stable environments may be combined in a single set of curves in spite of the use of Gaussian profiles in the neutral case and top-hat profiles in the stable case, a slightly different reduction of the equations will be used here. The environmental stability will be characterized by the Brunt–Väisälä frequency N, where $N^2 = -(g/\rho_0)\,d\rho_e/dx = \beta g\,dT_e/dx$ and $\beta = T_0^{-1}$ is the coefficient of expansion. The conservation equations for a stable environment reduce under transformations

$$V = bU, \quad W = b^2U, \quad F = b^2uP$$

and
$$F = |F_0|f, \quad V = V_0 v, \quad W = \alpha^{\frac{1}{2}}\lambda^{-1}V_0^{\frac{5}{2}}|F_0|^{-\frac{1}{2}}w,$$
$$X = 2^{-1}\alpha^{-\frac{1}{2}}\lambda^{-1}V_0^{\frac{3}{2}}|F_0|^{-\frac{1}{2}}x,$$

to the forms
$$\frac{dw}{dx} = v, \quad \frac{dv^4}{dx} = fw, \quad \frac{df}{dx} = -\Delta w,$$

where $\Delta = N^2V_0^4/2\lambda^2F_0^2$; and the corresponding boundary conditions at $x = 0$ are

$$v = 1, \quad f = \operatorname{sgn}\Gamma, \quad w = 2^{\frac{9}{4}}5^{-\frac{1}{2}}\lambda(1+\lambda^2)^{-\frac{1}{2}}|\Gamma|^{\frac{1}{2}} = 2^{\frac{3}{2}}5^{-\frac{1}{2}}|\Gamma'|^{\frac{1}{2}}.$$

Thus, provided that $\Gamma' = 2^{\frac{3}{2}}\lambda^2(1+\lambda^2)^{-1}\Gamma$ is used in place of Γ, the equations and boundary conditions for Gaussian plumes in a neutral environment and top-hat plumes in a stable environment correspond, and the two sets of results are directly compatible.

The behaviour of forced plumes in a stably stratified environment depends on the source strength (F_0, V_0, W_0) and on ambient stability, here represented by N.

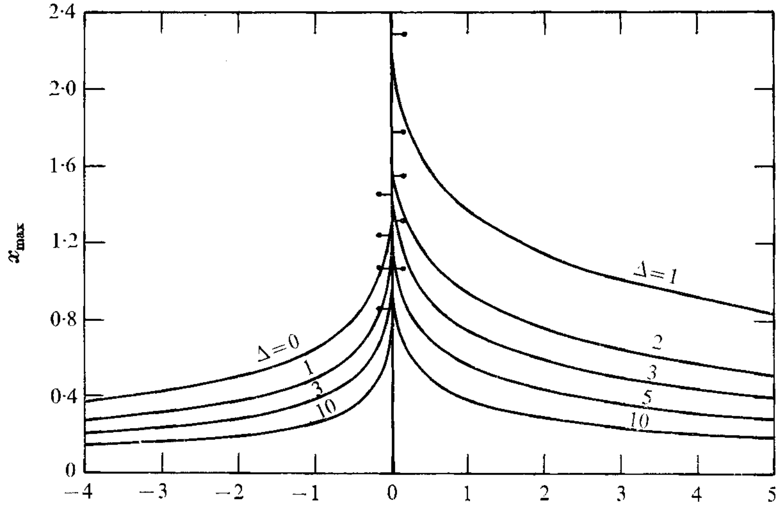

FIGURE 5. A scale diagram for the ascent of forced plumes in a uniform environment showing maximum heights of ascent for plumes with physical sources at the level $x = 0$. This form of diagram applies especially for families of plumes having constant momentum and buoyancy fluxes from the source (V_0, F_0), and in this case $\Gamma \propto W_0^2$ for neutral environments, $\Gamma' \propto W_0^2$ for stable environments (and differs by a constant of proportionality from Γ to allow for differences in assumed profile shape) and $\Delta \propto N^2$, where W_0 is proportional to the mass flux from the source and N is the Brunt–Väisälä frequency for the environment. Γ and Γ' are positive for plumes with upward buoyancy and negative for those emitted upwards but with negative buoyancy.

Only two of the four quantities F_0, V_0, W_0 and N are needed as a transformation base to reduce the governing equations to non-dimensional form, and it follows that two non-dimensional parameters can be formed to characterize flow states. It is thus apparent that there are six different transformations of the equations to non-dimensional form, and that the two-parameter family of solutions will exhibit a very wide range of flow behaviour. The particular choice of transformation depends on the particular application: (i) Morton (1959) was concerned with ways of emitting a specified heat flux into a given environment, and so based his transformation on the flux of buoyancy from the source F_0 and the ambient stability N ($\equiv G$); (ii) if the initial flux of buoyancy plays a minor role because of strong stratification the appropriate transformation base is (V_0, N); and (iii) in the present treatment the base (F_0, V_0) is taken as representing the forcing at the actual source. Once the transformation base has been selected, it is convenient to construct a dimensionless parameter from each of the remaining two quantities in combination with those of the transformation base. In the present case these are $\Delta = N^2V_0^4/2\lambda^2F_0^2$, involving N, and $\Gamma' = 5\lambda^2F_0W_0^2/8\alpha V_0^5$, involving W_0, and the family of solutions for a specified 'strength' (F_0, V_0) is investigated over a range of values of Δ, representing environmental stability, and Γ', representing mass flux from the source.

The behaviour of forced plumes generated by upward emission $(W_0, V_0 > 0)$ of either positively or negatively buoyant fluid $(F_0 \gtrless 0)$ into a stably stratified

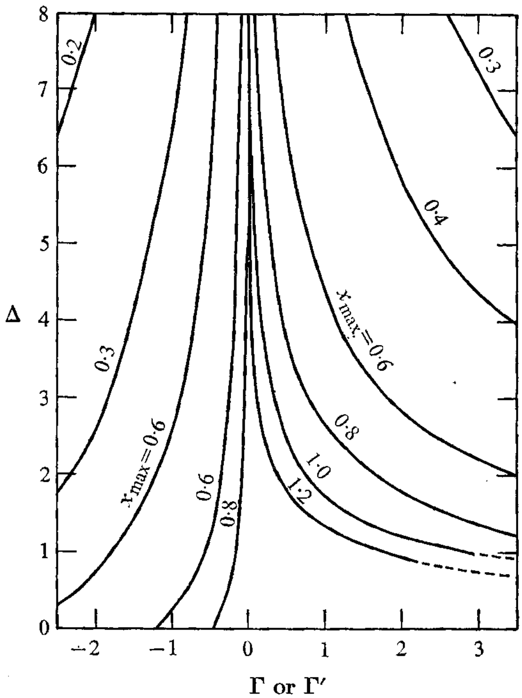

FIGURE 6. Contours of equal height x_{max} for the ascent of forced plumes from sources Γ in stable environments Δ, where Γ (for neutral environments) and Γ′ (for stable environments) are proportional to $F_0 W_0^2/V_0^5$ and $\Delta \propto N^2 V_0^4/F_0^2$.

environment (N real) is illustrated in figures 5 and 6. Here V_0 and F_0 are regarded as specified for a series of sources with different mass fluxes W_0 and environments N, and Γ (or Γ′) and Δ are used to specify the source and the environment, respectively. One of the most significant features of forced-plume behaviour in a stable environment is the maximum height of ascent x_{max} above the source, and figures 5 and 6 give two forms of dimensionless *scale diagram* for these ascent heights. Figure 5 shows a family of curves of x_{max} against Γ (for neutral environments) or Γ′ (for stable environments), each corresponding to a particular value of the stability parameter Δ. At constant V_0 and F_0, Γ or $\Gamma' \propto W_0^2$ with the result that an increase in Γ or Γ′ implies an increase in source radius together with decreases in source velocity and excess temperature; thus forced plumes with large $|\Gamma|$ or $|\Gamma'|$ have rather small heights of ascent, $2^{-1}\alpha^{-\frac{1}{2}}\lambda^{-1} V_0^{\frac{3}{2}}|F_0|^{-\frac{1}{2}} x_{max}$, in relation to those with small $|\Gamma|$ or $|\Gamma'|$. Naturally, forced plumes with positive buoyancy, $\operatorname{sgn} \Gamma' = +1$, rise higher than those with negative buoyancy. The ascent heights for Γ, $\Gamma' = 0$ are finite and are marked to right and left of the x axis for the limiting cases of positively buoyant and negatively buoyant plumes, respectively. Figure 6 shows a family of contours of equal x_{max} in a Γ, Δ frame, and for specified Δ and x_{max} there is just one source of positive buoyancy and one source of negative buoyancy that will achieve the desired penetration. This family of ascent height contours may be used to select appropriate sources for desired heights of penetration in specified environments.

It may be noted that Morton (1959) used a plotting co-ordinate $\Delta/(1+\Delta)$ rather than Δ as a device to telescope the less interesting sections of a solution curve at large Δ, and also that the initial reduction in total height of rise of a plume when the source momentum flux is increased is less obvious though still present in this representation. The various different representations involve quite different transformations and hence different scaling of the variables, and so serve to emphasize different aspects of forced-plume behaviour.

This work was carried out while BRM was on leave at the Department of Earth and Planetary Sciences, the Johns Hopkins University. Support by the National Science Foundation under grant GA-16603 is gratefully acknowledged.

REFERENCES

ABRAHAM, G. 1967 Jets with negative buoyancy in homogeneous fluids. *J. Hydraulic Res.* **4**, 235–248.

MORTON, B. R. 1959 Forced plumes. *J. Fluid Mech.* **5**, 151–163.

MORTON, B. R. 1971 The choice of conservation equations for plume models. *J. Geophys. Res.* **76**, 7409–7416.

ROUSE, H., YIH, C. S. & HUMPHREYS, H. W. 1952 Gravitational convection from a boundary source. *Tellus*, **4**, 201–210.

TELFORD, J. W. 1966 The convective mechanism in clear air. *J. Atmos. Sci.* **23**, 652–666.

TURNER, J. S. 1969 Buoyant plumes and thermals. *Ann. Rev. Fluid Mech.* **1**, 29–44.